

Finite-Bias Cooper Pair Splitting

L. Hofstetter,¹ S. Csonka,^{1,2} A. Baumgartner,^{1,*} G. Fülöp,² S. d'Hollosy,¹ J. Nygård,³ and C. Schönenberger¹

¹*Department of Physics, University of Basel, Klingelbergstrasse 82, CH-4056 Basel, Switzerland*

²*Department of Physics, Budapest University of Technology and Economics, Budafoki u. 6, 1111 Budapest, Hungary*

³*Nano-Science Center, Niels Bohr Institute, University of Copenhagen, Universitetsparken 5, DK-2100 Copenhagen, Denmark*

(Received 12 May 2011; published 19 September 2011)

In a device with a superconductor coupled to two parallel quantum dots (QDs) the electrical tunability of the QD levels can be used to exploit nonclassical current correlations due to the splitting of Cooper pairs. We experimentally investigate the effect of a finite potential difference across one quantum dot on the conductance through the other completely grounded QD in a Cooper pair splitter fabricated on an InAs nanowire. We demonstrate that the nonlocal electrical transport through the device can be tuned by electrical means and that the energy dependence of the effective density of states in the QDs is relevant for the rates of Cooper pair splitting (CPS) and elastic cotunneling. Such experimental tools are necessary to understand and develop CPS-based sources of entangled electrons in solid-state devices.

DOI: 10.1103/PhysRevLett.107.136801

PACS numbers: 73.23.-b, 03.67.Bg, 73.63.Nm, 74.45.+c

The electrons of a Cooper pair in a conventional superconductor form a spin singlet, which might be exploited as a naturally occurring on-chip source of spin-entangled Einstein-Podolsky-Rosen (EPR) [1,2] electron pairs, if the electrons can be separated coherently [3–5]. This Cooper pair splitting (CPS) can be understood as inverse crossed Andreev reflection, which is extensively investigated in metallic nanostructures with tunnel contacts [6–10]. However, other processes like elastic cotunneling (EC) make the detection of CPS difficult. It has been suggested to use electrically tunable quantum dots (QDs) coupled to a superconducting lead to obtain a better tunability of the electron-electron interactions relevant in these processes [3,5]. Recently, first transport characteristics at zero bias were reported for InAs nanowire (NW) and carbon nanotube QD devices, which are explained by CPS [11,12].

The bias-tunable nonlocal resistance in metallic structures was attributed to the excitation of different modes of the electromagnetic environment by CPS and EC [7,9,10,13,14]. This environment, however, is difficult to control experimentally. Applying independent electrical potentials to all three terminals of a Cooper pair splitter in conjunction with correlation measurements can be used to identify the relevant processes [10,15]. Here we report finite-bias differential conductance measurements on InAs nanowire devices similar to those in Ref. [11]. We show that the conductance through one QD is not entirely due to local processes, but also due to nonlocal higher order tunneling, consistent with a simple picture of CPS and EC. Since these processes depend differently on the bias, the relative rates can be tuned by external means. In particular, we show that the energy dependent effective density of states (DOS) due to the QD levels is crucial for the reported effects.

A colored SEM image of a generic CPS device is shown in Fig. 1(a). An InAs wire [16] is contacted by a

superconducting strip in the center (*S*) and two Ti/Au normal metal leads (*N1*, *N2*), which define two quantum dots QD1 and QD2. The two top-gates (*g1*, *g2*) are strongly decoupled from each other, so that the QD levels can be tuned individually, while the highly-doped Si wafer separated from the device by 400 nm thermal oxide serves as a global back-gate. More details on the sample fabrication can be found in [11]. All experiments were performed at the base-temperature of $T \approx 20$ mK.

Also shown in Fig. 1(a) is the measurement schematic: an ac voltage of $dU = 10 \mu\text{V}$ at 77 Hz is applied to the superconductor at zero dc potential. A dc voltage U_{N2} is applied to contact *N2* of QD2, while a home-built current-voltage converter (gain 10^8 V/A) and a standard lock-in amplifier are used to measure the ac current I_1 in contact *N1* from QD1. A $10 \mu\text{F}$ capacitor *C* ensures that *N1* and *S* are at the same dc potential, in spite of possible IV converter offset voltages [17]. Figure 1(b) shows the energy diagram of such a device.

To characterize QD1, the differential conductance $G_1 = dI_1/dU$ is plotted in Fig. 2(a) as a function of the gate voltage U_{g1} and the bias applied to *N1*, U_{N1} . We observe

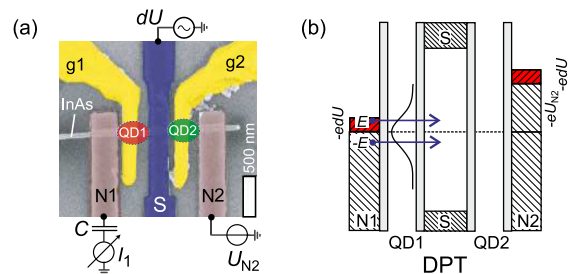


FIG. 1 (color online). (a) Colored SEM image of a typical device and measurement circuitry. (b) Schematics of direct Cooper pair tunneling (DPT) with an ac voltage dU imposed on QD1 and QD2 and a finite bias U_{N2} across QD2.

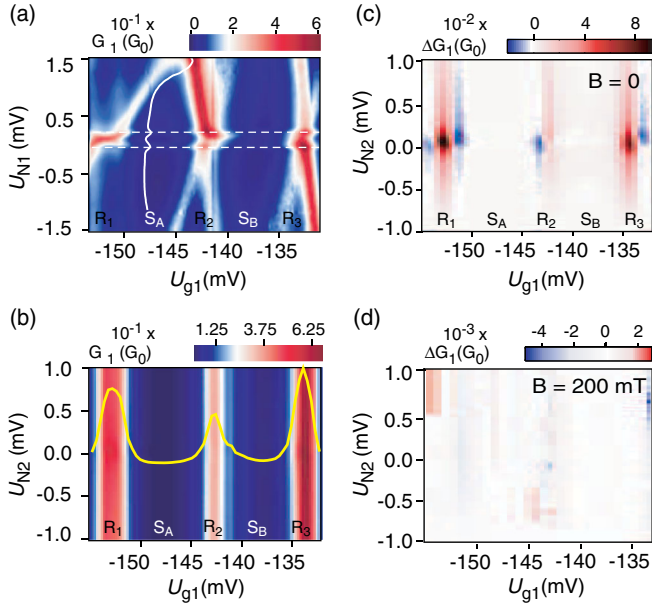


FIG. 2 (color online). (a) Characterization of QD1: differential conductance G_1 as a function of U_{N1} and U_{g1} at $B = 0$. The cross section shows two small features related to the superconductor gap Δ . (b) G_1 as a function of U_{N2} and U_{g1} at $B = 0$. (c) $\Delta G_1 = G_1(U_{g1}, U_{N2}) - G_1(U_{g1}, U_{N2} = -1 \text{ mV})$ derived from the data in (b) for the same parameter range. (d) ΔG_1 for the same experiment at $B = 200 \text{ mT}$.

well-defined Coulomb blockade oscillations consistent with the formation of a QD [18]. We label the resonances in the figure as $R_1 - R_3$ and the electronic states in-between as S_A and S_B , from left to right. From this plot we extract various sample parameters, e.g., the superconducting gap $\Delta \approx 130 \mu\text{eV}$ (cross section at $U_{g1} = -0.146 \text{ V}$), or an addition energy of $\sim 3 \text{ meV}$ and a tunnel coupling of $\Gamma \approx 500 \mu\text{eV}$ for S_B . We note that $\Gamma > \Delta$ so that sequential tunneling of the Cooper pair electrons is not suppressed entirely. In addition, a split Kondo resonance [18,19] in S_B can be observed around zero bias in the normal state data when the superconductivity is suppressed by an external magnetic field (not shown). A similar characterization of QD2 in the parameter range of the experiments (not shown) exhibits only small variations in the conductance. In the discussion below we therefore assume a resonance in the effective DOS of QD1 and a constant DOS for QD2, as illustrated in Fig. 1(b).

The dominant component of I_1 is due to local transport processes between S and N_1 . As an example, direct Cooper pair tunneling (DPT), also known as Andreev reflection, is illustrated in Fig. 1(b): applying the voltage dU to S as in the experiment is equivalent to applying $-dU$ to $N1$ and $N2$. An electron at energy E and one at $-E$ are injected from $N1$ to form a Cooper pair in S . Because S and N_1 are at the same dc potential, all local transport processes are independent of the voltage U_{N2} on $N2$, if charge imbalance [14] and local heating can be neglected. Therefore only “nonlocal” transport processes, which comprise correlated

coherent tunneling of electrons through QD1 and QD2, can lead to a dependence of I_1 on U_{N2} .

Figure 2(b) shows G_1 as a function of the top-gate voltage U_{g1} of QD1 and the bias U_{N2} applied to QD2. On this scale the conductance seems independent of U_{N2} . We assume that all nonlocal processes become ineffective at $U_{N2} \gg \Delta/e$ and therefore plot in Fig. 2(c) the deviation of G_1 from a high-bias value, $\Delta G_1(U_{g1}, U_{N2}) = G_1(U_{g1}, U_{N2}) - G_1(U_{g1}, U_{N2} = -1 \text{ mV})$. We note that the color scale is adjusted to white representing $\Delta G_1 = 0$. For the gate voltage U_{g1} tuned to resonance R_1 , ΔG_1 has a positive maximum at zero bias with $\Delta G_1/G_1 \approx 15\%$. The extent of this maximum is roughly $eU_{N2} \approx \Delta$ and $e\alpha U_{g1} \approx \Gamma$ (α : lever arm of top gate $g1$). With U_{g1} slightly off-peak, a minimum in ΔG_1 occurs on both sides of resonance R_1 , but *not* centered around $U_{N2} = 0$. These features will be examined in more detail below. Similar features occur on the resonances 2 and 3, however without minima where state B is involved.

In a control experiment the superconductivity is suppressed by an external magnetic field of 200 mT parallel to the Al strip. The corresponding plot of ΔG_1 is shown in Fig. 2(d). No clear structure can be discriminated, though the scale is considerably smaller than in Fig. 2(c). We therefore conclude that the features in Fig. 2(c) are due to the superconductor and nonlocal transport processes, which become unlikely if S is in the normal-conducting state.

Figure 3 shows cross sections $\Delta G_1(U_{N2})$ of Fig. 2(c). The corresponding top-gate voltages U_{g1} are near resonance 1 and indicated on the zero-bias top-gate sweep $G_1(U_{g1})$ in Fig. 3(a). For gate voltages far from the resonance the bias dependence of ΔG_1 shows a small but pronounced minimum at zero bias, as shown in Figs. 3(b) and 3(g), while on resonance a strong peak is observed at zero bias, see Fig. 3(d). Zero bias across QD2 is indicated by dashed vertical lines in all plots and is slightly offset due to a small input offset voltage from an IV-converter mounted on lead $N2$. Slightly off-resonance the bias dependence is asymmetric with respect to zero bias: in Fig. 3(c) ΔG_1 exhibits a minimum at negative and a maximum at positive bias, while on the other side of the resonance a maximum can be found at negative and a minimum at positive bias; see Figs. 3(e) and 3(f). We note that the maxima and minima near the resonance are not at zero bias, whereas far off the resonance only a minimum at $U_{N2} = 0$ is found.

The nonlocal signals decay with increasing temperature, as shown in the inset of Fig. 3(a) for the conductance minimum at $U_{g1} = -0.1485 \text{ V}$, essentially the gate position of Fig. 3(g). The amplitude of ΔG_1 decreases monotonically and disappears at $T \approx 175 \text{ mK}$. Up to this temperature we have found no significant change in the superconductor gap. We therefore conclude that Δ is not the limiting energy scale in this problem, reminiscent of the CPS observed in [11] at zero bias.

A qualitative understanding of the experiments can be gained by expressing the CPS and EC tunneling rates by energy dependent effective density of states $D_1(E)$ and $D_2(E)$ in QD1 and QD2, incorporating the respective QD transmissions. The processes are illustrated in Fig. 4, for which we assume a resonance feature for D_1 and a constant for QD2, i.e. $D_2(E) = D_2$. We neglect changes in the DOS by virtual tunneling processes [20] and electron-electron interactions in the QDs and the leads.

The probability that an electron from QD1 at energy E and one from QD2 at energy $-E$ form a Cooper pair in S (inverse CPS) depends on the DOS as

$$\propto M_{\text{CPS}}(E)D_1(E)D_2(-E)f(E, \mu_1)f(-E, \mu_2), \quad (1)$$

with the respective electrochemical potentials $\mu_{1,2}$ in the leads, measured relative to the $\mu_S = 0$ in the superconductor. M_{CPS} represents the transition probability. For CPS the states of the QDs have to be empty initially and the Fermi functions $f(\pm E, \mu_{1,2})$ are replaced by $1 - f(\pm E, \mu_{1,2})$. We note that generally we have inverse CPS for $U_{N2} < 0$ and CPS for $U_{N2} > 0$. The situation for EC is shown schematically in Fig. 4(b). Since the process is elastic, its probability at the energy E scales as

$$\propto M_{\text{EC}}(E)D_1(E)D_2(E)[f(E, \mu_2) - f(E, \mu_1)]. \quad (2)$$

Summation over all energies for periodically varying U_{N1} and U_{N2} results in the nonlocal (nl) differential conductance, $\Delta G_1 = dI_{1,\text{nl}}/dU$. Assuming that M_{CPS} , M_{EC} and D_2 are independent of E , as well as $T \rightarrow 0$ and $edU \ll \Gamma$, the following intuitive expressions for the contributions of

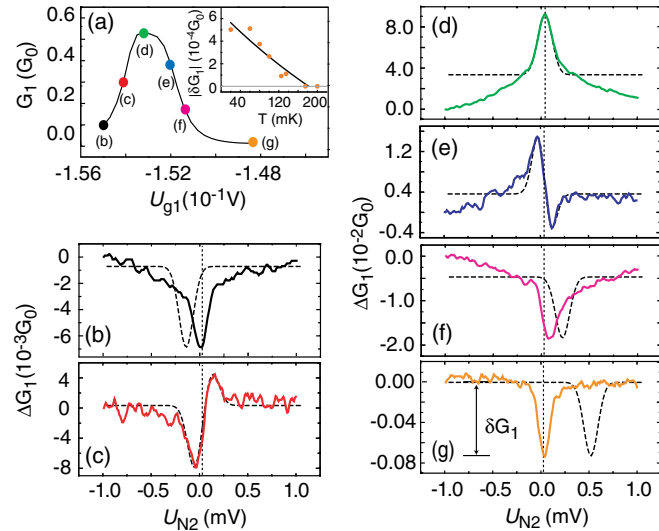


FIG. 3 (color online). Bias dependence of ΔG_1 for a series of top-gate voltages U_{g1} . The latter are indicated in (a). The dashed curves are derived from the model discussed in the text. Vertical lines indicate $U_{N2} = 0$, including a small offset from the IV-converter on $N2$. The inset in (a) shows the temperature dependence of the minimum in (g) with a black line as a guide to the eye.

CPS (G_{CPS}) and EC (G_{EC}) to $\Delta G_1 = G_{\text{CPS}} + G_{\text{EC}}$ can be found:

$$G_{\text{CPS}} = \frac{e^2}{h} M_{\text{CPS}} D_2 [D_1(0) + D_1(+eU_{N2})] \quad (3)$$

$$G_{\text{EC}} = \frac{e^2}{h} M_{\text{EC}} D_2 [D_1(0) - D_1(-eU_{N2})] \quad (4)$$

Both processes have a component from the DOS at $E = 0$. In addition, CPS has a positive contribution from D_1 at $+eU$, while EC has a negative contribution from $-eU$. This can also be understood from the diagrams in Fig. 4. We note that in our measurement scheme the differential conductance due to EC would be zero for energy independent transmissions, e.g., in metallic structures, and the contribution of CPS would be constant and independent of the bias applied to $N2$.

First we discuss the case when QD1 is tuned to a symmetric resonance, i.e. $D_1(E) = D_1(-E)$ and $D_1(0) > D_1(E \neq 0)$, as depicted in Figs. 4(a) and 4(b). From Eqs. (3) and (4) one finds that G_{CPS} has a maximum and G_{EC} a minimum with $G_{\text{EC}} = 0$ at $U_{N2} = 0$. Both signals are positive on a resonance. If the two processes had the same probability, $M_{\text{CPS}} = M_{\text{EC}}$, the variations of G_{CPS} and G_{EC} would cancel exactly and we would not expect any changes in ΔG_1 as a function of U_{N2} . We therefore conclude that CPS and EC can obtain different relative weights and the comparison with the experiment in Fig. 3(d) suggests that on a resonance CPS is the dominant process, i.e. $M_{\text{CPS}} \gg M_{\text{EC}}$, independent of U_{N2} .

An off-resonance situation is illustrated in Figs. 4(c) and 4(d). If the resonance is shifted in energy to $E = E_0 = -e\alpha\Delta U_{g1}$ by top-gate 1 [$E_0 < 0$ in Figs. 4(c)

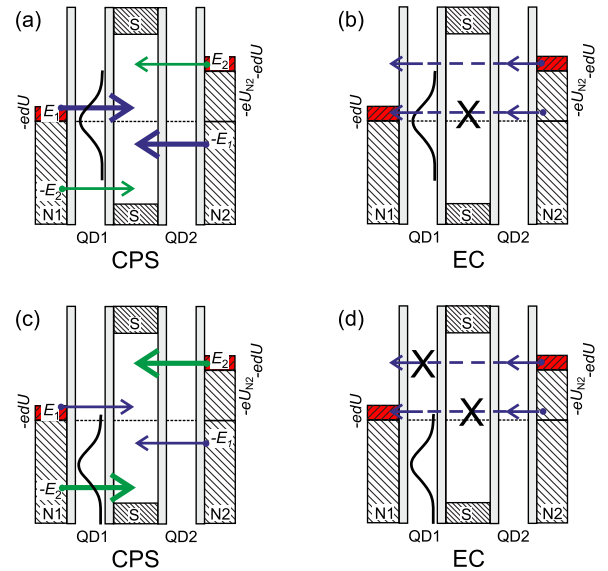


FIG. 4 (color online). Schematics of CPS and EC at finite bias on QD2 and an ac voltage dU imposed on both QDs. (a) and (b) show the situation when QD1 is tuned to a resonance, while (c) and (d) depict the case when the resonance is shifted to negative energies.

and 4(d)], Eqs. (3) and (4) predict two features: (i) Since $D_1(E_0) \gg D_1(0) > D_1(-E_0)$, one finds for $eU_{N2} = E_0$ that G_{CPS} has a positive maximum and dominates ΔG_1 ; (ii) similarly, one finds for $eU_{N2} = -E_0$ a negative minimum in both, G_{EC} and ΔG_1 , the latter because G_{CPS} is negligible. Such features are observed in Figs. 3(c) and 3(e), where a minimum and a maximum occur as a function of U_{N2} , with reversed order depending on the gate voltage relative to the resonance.

The results of numerical evaluations of Eqs. (2) and (3) with a Gaussian for D_1 and the adjustable parameters M_{CPS} , M_{EC} and an offset, leads to the dashed curves in Figs. 3(b)–3(g). The data are reproduced qualitatively near the resonance and we find that CPS is favored on resonance, while slightly off-resonance EC obtains a similar strength as CPS. These findings might be related to a reduction of CPS for energies close to Δ , while EC is increased due to the energy-dependence of the second order tunnel matrix elements. Both rates diminish above Δ due to the creation of excitations in S .

This model is very rudimentary and neglects electron-electron interactions in the leads and on the QDs, which might be crucial to understand details in our data. A strong indication for this is that in all Coulomb blockade regions a minimum occurs at zero bias, see Figs. 3(b) and 3(g), which cannot be reproduced in the model. The dashed curves in these figures are for $M_{\text{EC}} \gg M_{\text{CPS}}$ and show a minimum adjusted to the dip in the data, but at a wrong bias. A dip at zero bias, however, is in qualitative agreement with a zero-bias anomaly due to dynamical Coulomb blockade [9,10]. In addition, in state S_B , for which we observe Kondo correlations in the Coulomb diamonds, the minima in ΔG_1 expected near the resonances are missing or very weak, while they are clearly observed for the other states. This might be due to a competition between the superconducting and the Kondo correlations, which is not accounted for in our model.

In summary, we have reported finite-bias measurements on an InAs nanowire quantum dot Cooper pair splitter. Our results show that the energy dependent transmission due to the QDs has strong effects on nonlocal processes in such systems. We show that finite-bias spectroscopy is useful to identify nonlocal processes and find that Cooper pair splitting can be the dominant process on a QD resonance. Off-resonance we find a pattern consistent with EC being of similar strength as CPS. These findings are interpreted in a simple model based on energy dependent effective density of states. However, this model does not account for the relative strength of the processes, nor for features in the Coulomb blockade regions or where Kondo correlations are relevant. We tentatively attribute the latter findings to electron-electron interactions, which should be studied in greater detail to understand the involved mechanisms and find means to exploit them in an on-chip source of entangled electrons.

We thank Jens Schindele for fruitful discussions and acknowledge the financial support by the EU FP7 project SE²ND, the EU ERC project CooPairEnt, OTKA CNK80991, TAMOP 4.2.1./B-09/1/KMR-2010-2, the Swiss NCCR Nano and NCCR Quantum, the Swiss SNF, the Danish Research Councils and the Bolyai J. Scholarship for S.C.

Note added in proof.—During the review process we became aware of related theoretical works by Bursset, Herrera, and Levy-Yeyati [21].

*andreas.baumgartner@unibas.ch

- [1] A. Einstein, B. Podolsky, and N. Rosen, *Phys. Rev.* **47**, 777 (1935).
- [2] M.D. Reid, P.D. Drummond, W.P. Bowen, E.G. Cavalcanti, P.K. Lam, H.A. Bachor, U.L. Andersen, and G. Leuchs, *Rev. Mod. Phys.* **81**, 1727 (2009).
- [3] P. Recher, E. V. Sukhorukov, and D. Loss, *Phys. Rev. B* **63**, 165314 (2001).
- [4] G.B. Lesovik, T. Martin, and G. Blatter, *Eur. Phys. J. B* **24**, 287 (2001).
- [5] O. Sauret, D. Feinberg, and T. Martin, *Phys. Rev. B* **70**, 245313 (2004).
- [6] D. Beckmann, H.B. Weber, and H. v. Löhneysen, *Phys. Rev. Lett.* **93**, 197003 (2004).
- [7] S. Russo, M. Kroug, T.M. Klapwijk, and A.F. Morpurgo, *Phys. Rev. Lett.* **95**, 027002 (2005).
- [8] P. Cadden-Zimansky, J. Wei, and V. Chandrasekhar, *Nature Phys.* **5**, 393 (2009).
- [9] A. Kleine, A. Baumgartner, J. Trbovic, and C. Schönenberger, *Europhys. Lett.* **87**, 27011 (2009).
- [10] J. Wei and V. Chandrasekhar, *Nature Phys.* **6**, 494 (2010).
- [11] L. Hofstetter, S. Csonka, J. Nygård, and C. Schönenberger, *Nature (London)* **461**, 960 (2009).
- [12] L.G. Herrmann, F. Portier, P. Roche, A. Levy Yeyati, T. Kontos, and C. Strunk, *Phys. Rev. Lett.* **104**, 026801 (2010).
- [13] A. Levy Yeyati, F.S. Bergeret, A. Martín-Rodero, and T.M. Klapwijk, *Nature Phys.* **3**, 455 (2007).
- [14] A. Kleine, A. Baumgartner, J. Trbovic, D.S. Golubev, A.D. Zaikin, and C. Schönenberger, *Nanotechnology* **21**, 274002 (2010).
- [15] G. Bignon, M. Houzet, F. Pistolesi, and F.W.J. Hekking, *Europhys. Lett.* **67**, 110 (2004).
- [16] T.S. Jespersen, M. Aagesen, C. Sorensen, P.E. Lindelof, and J. Nygård, *Phys. Rev. B* **74**, 233304 (2006).
- [17] This is correct only for a strong coupling to the superconductor and if local processes are dominant, as it is the case in this device.
- [18] S. Csonka, L. Hofstetter, F. Freitag, S. Oberholzer, T.S. Jespersen, M. Aagesen, J. Nygård, and C. Schönenberger, *Nano Lett.* **8**, 3932 (2008).
- [19] D. Goldhaber-Gordon, H. Shtrikman, D. Mahalu, D. Abusch-Magder, U. Meirav, and M.A. Kastner, *Nature (London)* **391**, 156 (1998).
- [20] D. Chevallier, J. Rech, T. Jonckheere, and T. Martin, *Phys. Rev. B* **83**, 125421 (2011).
- [21] P. Bursset, W.J. Herrera, and A. Levy-Yeyati, arXiv:1104.3130v1 [Phys. Rev. B (to be published)].